



STRUCTURAL SCIENCE  
CRYSTAL ENGINEERING  
MATERIALS

Volume 77 (2021)

**Supporting information for article:**

**Structural effects of halogen bonding in iodothalcones**

**Victoria Hamilton, Connah Harris, Charlie L. Hall, Jason Potticary, Matthew E. Cremeens, Gemma D. D'Ambruoso, Masaomi Matsumoto, Stephen D. Warren, Natalie E. Pridmore, Hazel A. Sparkes and Simon R. Hall**

**S1. Characterization of chalcones****Table S1** Table of single crystal data for Ep2o.

<b>Identification code</b>	Ep2o
<b>Crystal data</b>	
Chemical formula	C <sub>15</sub> H <sub>10</sub> FIO
M <sub>r</sub>	352.13
Crystal system, space group	Monoclinic, P2 <sub>1</sub> /c
Temperature (K)	100
a, b, c (Å)	22.9802 (10), 4.7448 (2), 12.2026 (6)
β (°)	96.534 (2)
V (Å <sup>3</sup> )	1321.89 (10)
Z	4
Radiation type	Mo Kα
μ (mm <sup>-1</sup> )	2.42
Crystal size (mm)	0.48 × 0.28 × 0.18
<b>Data collection</b>	
Diffractometer	Bruker Apex II kappa CCD area detector
Absorption correction	Multi-scan SADABS2016/2 (Bruker,2016/2) was used for absorption correction. wR2(int) was 0.0623 before and 0.0413 after correction. The ratio of minimum to maximum transmission is 0.8124. The λ/2 correction factor is not present.
T <sub>min</sub> , T <sub>max</sub>	0.606, 0.746
No. of measured, independent and observed [I > 2σ(I)] reflections	10963, 3019, 2628
R <sub>int</sub>	0.031
(sin θ/λ) <sub>max</sub> (Å <sup>-1</sup> )	0.649
<b>Refinement</b>	
R[F <sup>2</sup> > 2σ(F <sup>2</sup> )], wR(F <sup>2</sup> ), S	0.024, 0.057, 1.05
No. of reflections	3019
No. of parameters	163
H-atom treatment	H-atom parameters constrained
Δρ <sub>max</sub> , Δρ <sub>min</sub> (e Å <sup>-3</sup> )	0.66, -0.52

**Table S2** Table of single crystal data for Ep2m.

Identification code	Ep2m
<b>Crystal data</b>	
Chemical formula	C <sub>15</sub> H <sub>10</sub> FIO
M <sub>r</sub>	352.13
Crystal system, space group	Triclinic, <i>P</i>
Temperature (K)	100
<i>a</i> , <i>b</i> , <i>c</i> (Å)	6.1200 (2), 10.7976 (3), 20.3875 (7)
α, β, γ (°)	103.101 (2), 95.160 (2), 98.186 (2)
<i>V</i> (Å <sup>3</sup> )	1288.32 (7)
<i>Z</i>	4
Radiation type	Mo <i>K</i> α
μ (mm <sup>-1</sup> )	2.48
Crystal size (mm)	0.43 × 0.29 × 0.16
<b>Data collection</b>	
Diffractometer	Bruker Apex II kappa CCD area detector
Absorption correction	Multi-scan SADABS2016/2 (Bruker,2016/2) was used for absorption correction. wR2(int) was 0.0644 before and 0.0421 after correction. The ratio of minimum to maximum transmission is 0.7438. The λ/2 correction factor is not present.
<i>T</i> <sub>min</sub> , <i>T</i> <sub>max</sub>	0.555, 0.746
No. of measured, independent and observed [ <i>I</i> > 2σ( <i>I</i> )] reflections	23620, 6172, 5279
<i>R</i> <sub>int</sub>	0.030
(sin θ/λ) <sub>max</sub> (Å <sup>-1</sup> )	0.660
<b>Refinement</b>	
<i>R</i> [ <i>F</i> <sup>2</sup> > 2σ( <i>F</i> <sup>2</sup> )], <i>wR</i> ( <i>F</i> <sup>2</sup> ), <i>S</i>	0.022, 0.051, 1.04
No. of reflections	6172
No. of parameters	325
H-atom treatment	H-atom parameters constrained
Δρ <sub>max</sub> , Δρ <sub>min</sub> (e Å <sup>-3</sup> )	0.92, -0.85

**Table S3** Table of single crystal data for Ep8p.

<b>Identification code</b>	Ep8p
<b>Crystal data</b>	
Chemical formula	C <sub>15</sub> H <sub>10</sub> INO <sub>3</sub>
M <sub>r</sub>	379.14
Crystal system, space group	Monoclinic, P2 <sub>1</sub> /c
Temperature (K)	100
a, b, c (Å)	17.9016 (7), 5.8824 (2), 25.4871 (9)
β (°)	94.427 (2)
V (Å <sup>3</sup> )	2675.89 (17)
Z	8
Radiation type	Mo Kα
μ (mm <sup>-1</sup> )	2.40
Crystal size (mm)	0.47 × 0.19 × 0.08
<b>Data collection</b>	
Diffractometer	Bruker Apex II kappa CCD area detector
Absorption correction	Multi-scan SADABS2016/2 (Bruker,2016/2) was used for absorption correction. wR2(int) was 0.0744 before and 0.0555 after correction. The ratio of minimum to maximum transmission is 0.7782. The λ/2 correction factor is not present.
T <sub>min</sub> , T <sub>max</sub>	0.581, 0.746
No. of measured, independent and observed [I > 2σ(I)] reflections	36371, 6154, 4831
R <sub>int</sub>	0.051
(sin θ/λ) <sub>max</sub> (Å <sup>-1</sup> )	0.649
<b>Refinement</b>	
R[F <sup>2</sup> > 2σ(F <sup>2</sup> )], wR(F <sup>2</sup> ), S	0.031, 0.072, 1.03
No. of reflections	6154
No. of parameters	361
H-atom treatment	H-atom parameters constrained
Δρ <sub>max</sub> , Δρ <sub>min</sub> (e Å <sup>-3</sup> )	0.92, -0.80

NMR data of synthesized chalcones obtained in CDCl<sub>3</sub>. Ep2o: 1H NMR (400 MHz, CDCl<sub>3</sub>) d 7.89 (m, 3H), 7.73 (d, 2H, J = 8.5 Hz), 7.63 (ddd, 1H, J = 7.6, 7.6, 1.6 Hz), 7.57 (d, 1H, J = 15.9 Hz), 7.39 (m, 1H), 7.20 (ddd, 1H, J = 7.6, 7.6, 0.9 Hz), 7.13 (ddd, 1H, J = 10.8, 8.3, 0.8 Hz). Ep2m: 1H NMR (400 MHz, CDCl<sub>3</sub>) d 7.87 (d, 2H, J = 8.5 Hz), 7.75 (m, 3H), 7.45 (d, 1H, J = 15.6 Hz), 7.39 (m, 2H), 7.34 (m, 1H), 7.12 (m, 1H).Ep2p: 1H NMR (400 MHz, CDCl<sub>3</sub>) d 7.86 (d, 2H, J = 8.5 Hz), 7.77 (d, 1H, J = 15.6 Hz), 7.72 (d, 2H, J = 8.5 Hz), 7.63 (m, 2H), 7.39 (d, 1H, J = 15.6 Hz), 7.11 (t, 2H, J = 8.6 Hz).Ep8p. 1H NMR (400 MHz, CDCl<sub>3</sub>) 7.56 (1H, d, 16 Hz), 7.70 – 7.85 (5H, m), 7.89 (2H, d, 8 Hz), 8.28 (2H, d, 12 Hz).

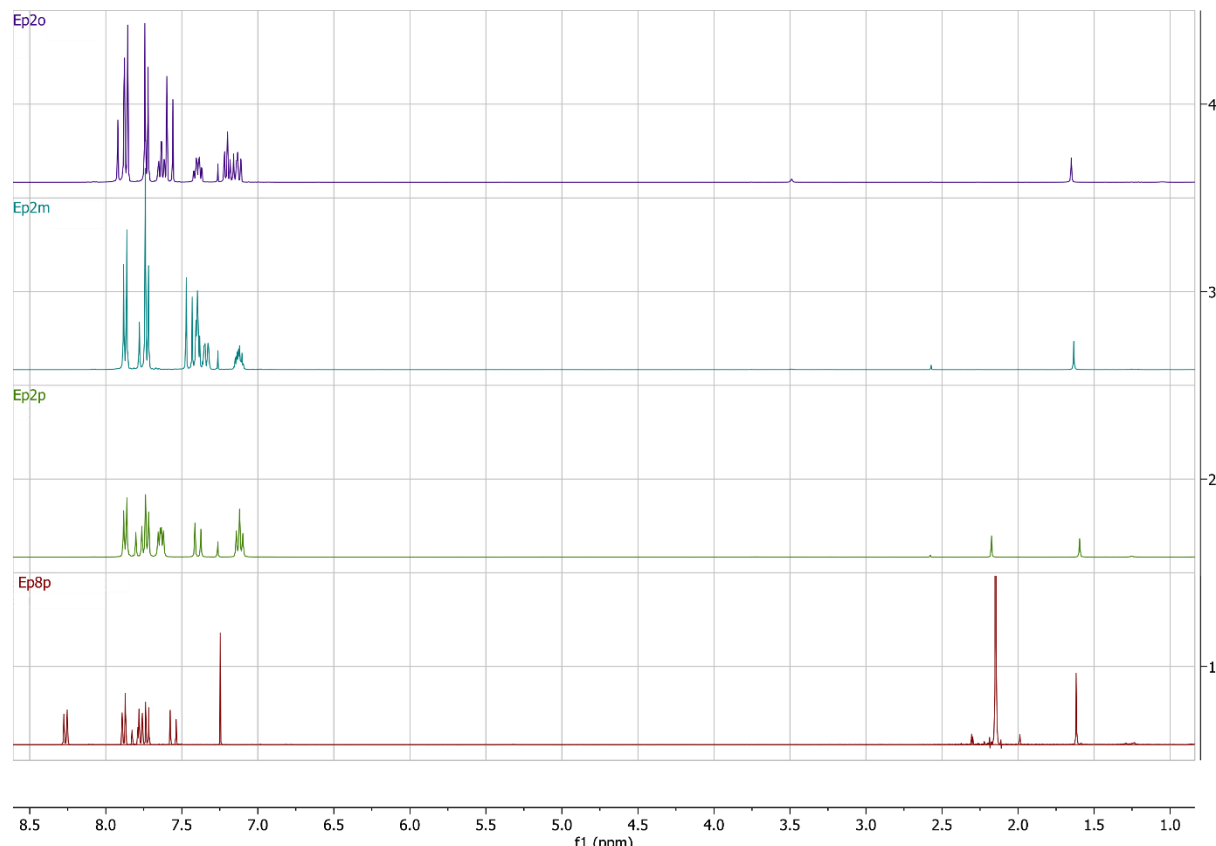


**Figure S1** 1H NMR spectra for (1) Ep8p, (2) Ep2p, (3) Ep2m and (4) Ep2o chalcones obtained in CDCl<sub>3</sub>.

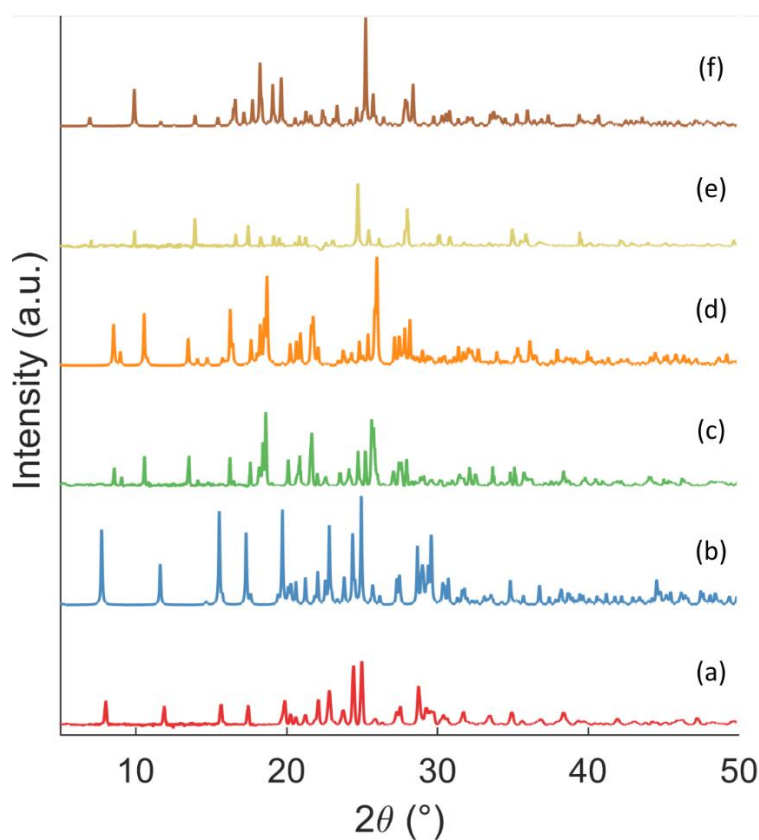


**Figure S2** Comparison of experimentally (exptal) obtained and simulated (sim) powder X-ray diffraction patterns for each of the solved chalcones structures: (a) Ep2o (exptal), (b) Ep2o (sim), (c) Ep2m (exptal), (d) Ep2m (sim), (e) Ep8p (exptal) and (f) Ep8p (sim). The absence of impurity peaks in the experimental data indicates phase purity.

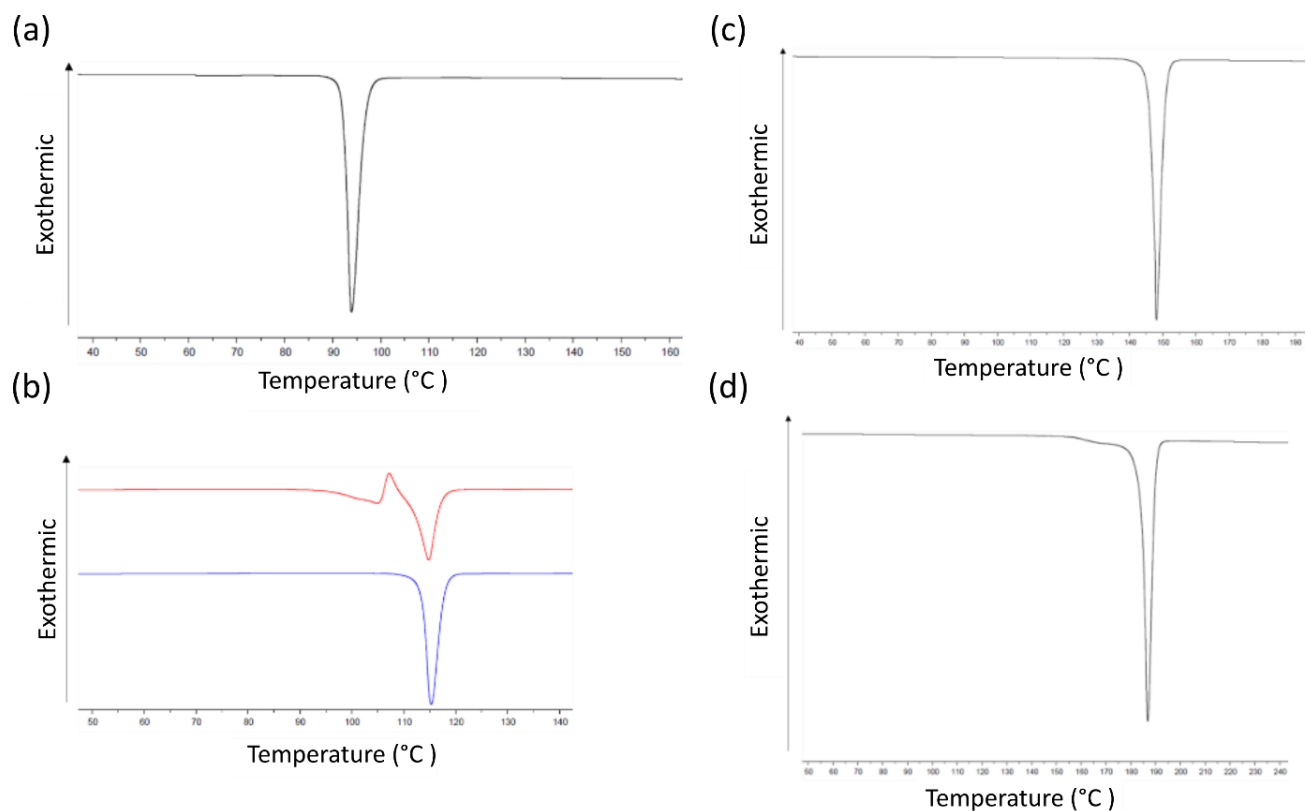


**Figure S3** Thermograms for (a) Ep2o, (b) Ep2pm rhomb crystals (blue) and plate-like (red), (c) Ep2p and (d) Ep8p. All data were acquired from 5-10 mg of hermetically sealed sample in Tzero pans at a scan rate of 10 °C/min on a TA Instruments DSC 25 Discovery.

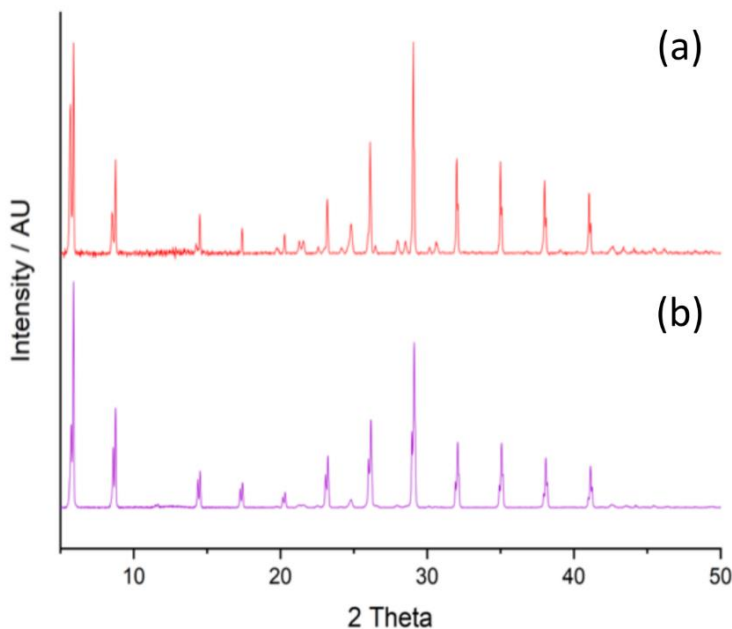


**Figure S4** Powder X-ray diffraction data from 5-50 2θ/° for (a) Ep2m plate-like polymorph (red) and (b) Ep2p plate-like crystals (purple) showing comparable diffraction patterns.

## S2. Molecular electrostatic potential surface maps

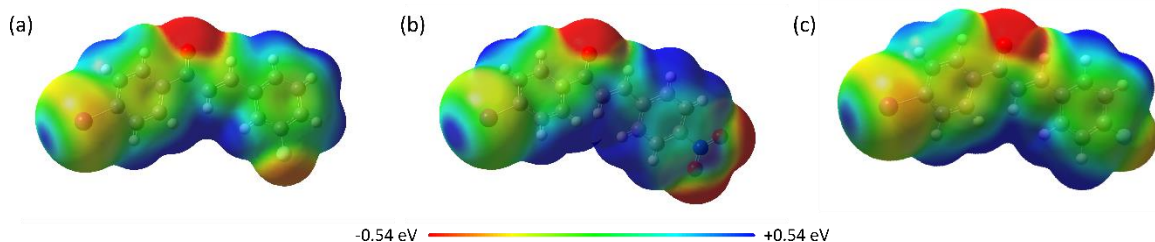


**Figure S5** Molecular electrostatic potential surfaces (MEPS) of the chalcones: (a) Ep2m-anti, (b) Ep8p-(2) and (c) an optimised geometry of Ep2p. The MEPS scale is the same for all, shown beneath, ranging from -0.54 eV to +0.54 eV, isovalue surface of  $0.004 \text{ e}\text{\AA}^{-3}$ . MEPS were created using Gaussian (Frisch *et al.*, 2009).

## S3. Electrostatic potential slices

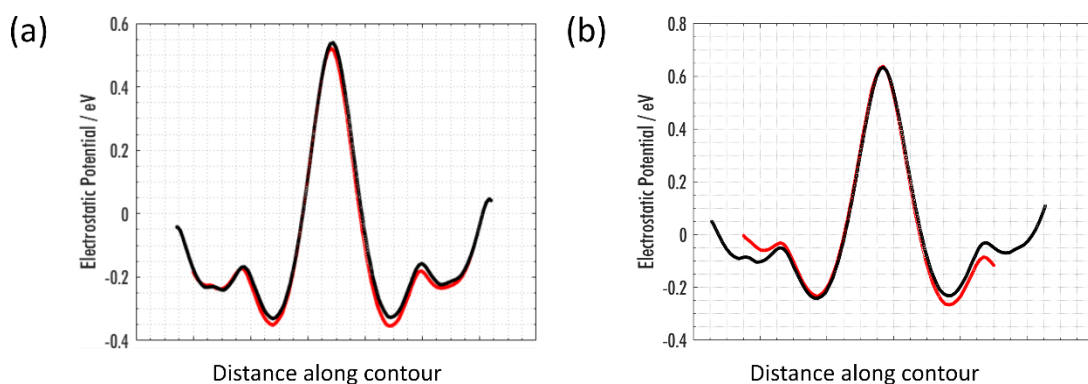


**Figure S6** Electrostatic potential slices along a contour running over the  $\sigma$ -hole of the iodine present in each the two molecules in the asymmetric unit cells of Ep2m -syn (black) and -trans (red) and Ep8p -(1) (black) and -(2) (red). Corresponding to the contours in Fig. 6.

## S4. Database analysis of aromatic iodine-iodine and iodine-nitro group halogen bonding

A database analysis was performed to find the frequency of iodine-nitro infinite linear chains, as observed in Ep8p and iodine channels, as observed in Ep2o, in related structures. Contour density surfaces were created from 3D scatterplots to find the frequency of occurrences of non-bonding contacts, data were pulled from the Cambridge Structural Database (CSD) using the program Isostar (Groom *et al.*, 2016; Bruno *et al.*, 1997). Interactions were limited to those whose contacts were shorter than the sum of the van der Waals radii, as larger than this is unlikely a halogen bond (Mukherjee *et al.*, 2014). The colours of the contour plot indicate the spatial density of contacts in that

position; the surface colours are auto-scaled from the maximum density displayed as red (100-75% of maximum density), green (75-50% of maximum density) and blue shows regions of low density (50-25% of maximum density).

For the aromatic I $\cdots$ O<sub>2</sub>N XB, 140 structures were found, density contour surface shown in Fig. S7(a) clearly showing how directional this bonding motif is with almost all contacts in-line with the aromatic iodine axis.

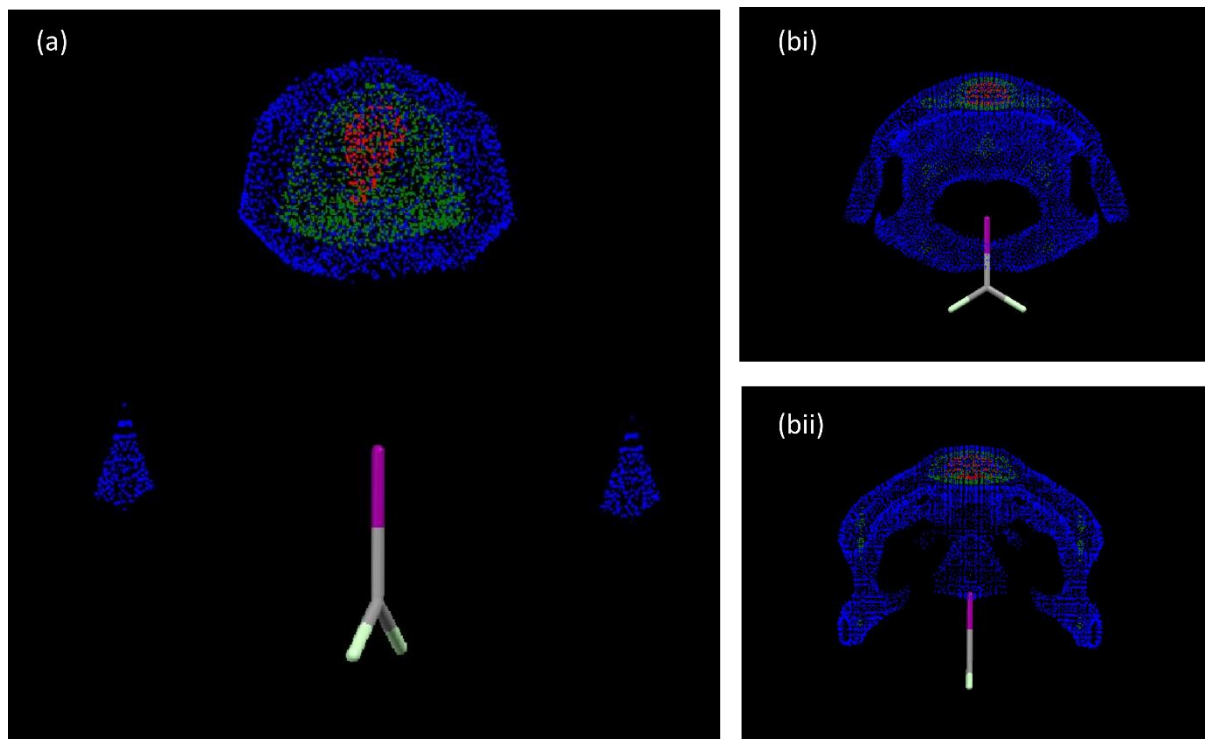


**Figure S7** Density contour surfaces of the frequency of positions of contacts around the probe molecule, an aromatic iodine contacts to within the van der Waals radii, containing (a) a nitro group and (b) to any C-I at (i) planar view and (ii) rotated orthogonally to this. Contour point colours are automatically generated and are proportionately scaled from the densest red (100-75% of maximum density) to medium density green (75-50% of maximum density) and lowest density blue (50-25% of maximum density). Contour surfaces were created using the program IsoStar with data obtained from the CSD (Bruno *et al.*, 1997; Groom *et al.*, 2016).

Using an aromatic substituted iodine as the probe molecule and limiting the search to include molecules under 900 daltons, only 11 unique structures were found to meet the criteria of a planar bond of the iodine with both oxygens (CSD-WUGVUR, -SUNGIT, -ITNOBE01, -MEZGIH, -ZONYIK, -WAWFUW, -LEPPPEC, -QEXZOK, -RAYCID03, -FEXCUH, -TAPMUT) (Groom *et al.*, 2016). The structures were evenly split between a simple benzene substituted with both iodine and nitro functional groups and those with benzene rings at either end of the molecule one with iodine

functionalisation and the other with nitro. This is a good indication of the conditions required for the formation of an infinite linear chain.

The I···I database search provided a larger challenge with the number of aromatic-I with any C-I bonds giving over 1000 possible structures within the van der Waals radii, Fig. S7(b). In Fig. S7(bi) and (bii) which are shown in plane with the aromatic ring and orthogonally to this, here the density contour plots show stark absences in orientations of contacts. These absences in contacts occur when C-I contacts are XBing to the probing aromatic iodine, these absences occur in bands at a contact angle of 90° when edge on to the plane of the aromatic ring and the reverse just above this band when at a contact angle roughly between 45–90°.

When searching for amphoteric I···I channels only 67 molecules fitting these criteria were found. When forming channels, these had a strong tendency towards the symmetrical bonds of equivalent lengths, with only six of these structures investigated displaying asymmetrical bonding (CSD-ZIYJUO, -SIXPEW, -XIZTEH, -ETOJUS02, -TAGYIM, -POPLAJ). Unlike HBs this tendency towards symmetry of XB<sub>s</sub> is well known for three centre XB<sub>s</sub> and XB in solution (Reiersølmoen *et al.*, 2020; Carlsson *et al.*, 2012). The majority of these formed simple alternating iodine channels, as observed for Ep2o.

### S5. Uncommon amphoteric iodine-iodine halogen bond motifs

The uncommon motifs from the database search are shown in Fig. S8. Simple single iodine channel per molecule can be grouped with those molecules with iodine channels presenting at both ends of a symmetrical molecule, Fig. S8(a). Rarely, each iodine in the channel also bonds to an additional adjacent iodine, in all instances these molecules present multiple iodine XB<sub>s</sub> (CSD-GAPVAU, -HINKEW, -PERCUM, -BOLNOG) (Groom *et al.*, 2016), Fig. S8(b). I···I amphoteric channels are also capable of forming more interesting structures, forming a square spiral iodine channel (CSD-BOPDOZ) (Groom *et al.*, 2016) and a rhombohedral channel (CSD-TAGYIM) (Groom *et al.*, 2016), Fig. S8(c) and (d), respectively. These more complex bonding patterns tend to be simpler rigid benzene or azulene-like structures with fewer functional groups, this is likely what allows iodine XB to dominate the crystal structure.

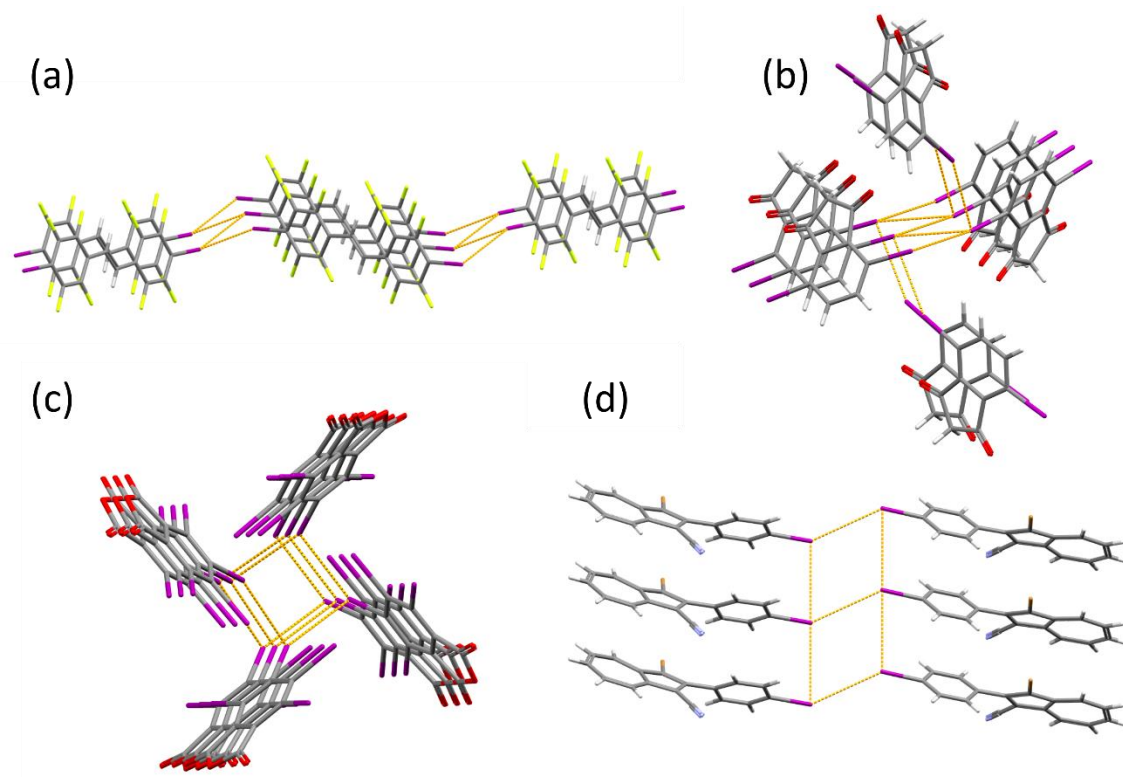


**Figure S8** Uncommon channels of amphoteric I...I channels for small molecules: (a) iodine channels at either end of a molecule, (b) iodine channel with adjacent bonding, (c) a square spiral channel and (d) a rhombohedral channel. CSD-MAGGUZ, -HINKEW, -BOPDOZ and -TAGYIM, respectively. Halogen bonds are shown by orange dashed lines, hydrogen bonds have been removed for clarity. Images were created using Mercury (Macrae *et al.*, 2008).

## References

- Bruno, I. J., Cole, J. C., Lommerse, J. P. M., Rowland, R. S., Taylor, R. & Verdonk, M. L. (1997). *J. Comput. Aided. Mol. Des.* **11**, 525-537.
- Carlsson, A. C. C., Gräfenstein, J., Budnjo, A., Laurila, J. L., Bergquist, J., Karim, A., Kleinmaier, R., Brath, U. & Erdélyi, M. (2012). *J. Am. Chem. Soc.* **134**, 5706-5715.
- Mukherjee, A., Tothadi, S. & Desiraju, G. R. (2014). *Acc. Chem. Res.* **47**, 2514-2524.
- Reiersølmoen, A. C., Battaglia, S., Øien-ØDegaard, S., Gupta, A. K., Fiksdahl, A., Lindh, R. & Erdélyi, M. (2020). *Chem. Sci.* **30**, 7979-7990.